J. Neurovirol. (2011) 17:353–367
DOI 10.1007/s13365-011-0041-6

The type I interferon response bridles rabies virus infection and reduces pathogenicity

Damien Chopy · Claudia N. Detje · Mireille Lafage · Ulrich Kalinke · Monique Lafon

Received: 25 March 2011 / Revised: 25 May 2011 / Accepted: 10 June 2011 / Published online: 30 July 2011

Abstract Rabies virus (RABV) is a neurotropic virus transmitted by the bite of an infected animal that triggers a fatal encephalomyelitis. During its migration in the nervous system (NS), RABV triggers an innate immune response, including a type I IFN response well known to limit viral infections. We showed that although the neuroinvasive RABV strain CVS-NIV dampens type I IFN signaling by inhibiting IRF3 phosphorylation and STAT2 translocation, an early and transient type I IFN response is still triggered in the infected neuronal cells and NS. This urged us to investigate the role of type I IFN on RABV infection. We showed that primary mouse neurons (DRGs) of type I IFN(α/β) receptor deficient mice ($IFNAR^{-/-}$ mice) were more susceptible to RABV than DRGs of WT mice. In addition, exogenous type I IFN is partially efficient in preventing and slowing down infection in human neuroblastoma cells. Intra-muscular inoculation of type I IFNAR deficient mice [$IFNAR^{-/-}$ mice and NesCre ($^{+/-}$) IFNAR ($^{flox/flox}$) mice lacking IFNAR in neural cells of neuroectodermal origin only] with RABV reveals that the type I IFN response limits RABV dissemination in the inoculated muscle, slows down invasion of the spinal cord, and delays mortality. Thus, the type I IFN which is still produced in the NS during RABV infection is efficient enough to reduce neuroinvasiveness and pathogenicity and partially protect the host from fatal infection.

Keywords Type I interferon · Rabies virus · Nervous system · $IFNAR^{-/-}$ mice · NesCre ($^{+/-}$) IFNAR ($^{flox/flox}$) mice

Abbreviations

RABV	Rabies virus
NC	Nucleocapsid

Introduction

Rabies virus (RABV), a negative single strand RNA virus that belongs to the *Rhabdoviridae* family, is responsible for 55,000 human cases of fatal encephalomyelitis per year. This neurotropic virus has developed a unique strategy to disseminate in the host and accomplish its life cycle. After inoculation into the muscle by the bite of an infected animal, RABV enters into the NS at the neuromuscular junction or nerve spindles, replicates in cell bodies and

Electronic supplementary material The online version of this article (doi:10.1007/s13365-011-0041-6) contains supplementary material, which is available to authorized users.

D. Chopy · M. Lafage · M. Lafon
Département de Virologie Institut Pasteur,
Unité de Neuroimmunologie Virale
75015 Paris, France

D. Chopy · M. Lafage · M. Lafon
CNRS, URA 3015
F -75015 Paris, France

D. Chopy · M. Lafage · M. Lafon (✉)
Institut Pasteur, Unité de Neuroimmunologie Virale,
Département de Virologie
F-75015 Paris, France
e-mail: monique.lafon@pasteur.fr

C. N. Detje · U. Kalinke
Institute for Experimental Infection Research, TWINCORE,
Centre for Experimental and Clinical Infection Research, a joint venture between the Helmholtz Centre for Infection Research and the Medical School Hannover
Hannover, Germany

neurites, and propagates from one infected neuron to the next by exploiting retrograde axonal transport. This step-by-step transmission allows RABV to invade the spinal cord and brain before targeting the salivary glands from where it is transmitted to another organism through the infected saliva.

RABV viral signature such as the 5′ tri-phosphate ssRNA is detected by the Retinoic Inducible Gene-I (RIG-I) protein, leading to RIG-I activation and interaction with the mitochondrial protein interferon β (IFN-β) promoter stimulator-1 (IPS-1) (Faul et al. 2010; Hornung et al. 2006). In turn, IPS-1 triggers two main signaling pathways through the phosphorylation of the IFN Regulatory Factor 3 (IRF3) and the activation of Nuclear Factor-κB (NF-κB); those are respectively responsible for the expression of type I IFN and the inflammatory cytokines. Type I IFN binding to the IFN(α/β) receptor (IFNAR), a heterodimer consisting of the IFN(α/β) R1 and R2 chains, located on basically all nucleated cells triggers janus kinase 1 (JAK-1) and tyrosine kinase 2 (TYK-2) recruitment to the IFNAR. The two kinases phosphorylate the Signal Transducer and Activator of Transcription (STAT) 1 and 2 allowing STAT1 and 2 to form homo- and heterodimers. These complexes translocate into the nucleus and induce transcription of hundreds of IFN Stimulated Genes (ISG). Those ISG, like 2′–5′-oligoadenylate synthetase (OAS-1), and type I IFN as well, are known to exert their antiviral effect at different levels of the viruses' life cycle. In particular, they were found to inhibit viral RNA transcription/translation, to perturbate post-translational modification of viral proteins, and to alter the viral packaging (D'Agostino et al. 2009; Jolly 2011; McFadden et al. 2009; Sadler and Williams 2008; Trottier et al. 2005).

As in many viruses, RABV has evolved mechanisms to escape the host innate immune response. The N and the P proteins of RABV both contribute to counteract the type I IFN response (Chelbi-Alix et al. 2006; Rieder and Conzelmann 2009). The N protein limits RIG-I signaling (Masatani et al. 2010a, c), whereas the P protein inhibits IRF3 phosphorylation (Brzozka et al. 2005; Rieder et al. 2011), suppresses STAT1 nuclear translocation (Brzozka et al. 2006; Vidy et al. 2007), and sequesters in the cytoplasm an antiviral protein, the promyelocytic leukemia (PML) protein (Blondel et al. 2010). Despite these evasive mechanisms, it has been observed that human post-mitotic neurons infected with RABV still trigger type I IFN responses in the early stages of infection (Prehaud et al. 2005) and that IFN is still expressed in the NS as the infection progresses (Chopy et al. 2011; Johnson et al. 2006; Lafon et al. 2008). This addresses the question of the role of this residual IFN in the pathogenesis of RABV. Previous studies have described type I IFN either as a protective, neutral, or aggravating factor in RABV pathogenesis (Faul et al. 2008; Lafon et al. 2008; Lodmell et al. 1989; Marcovistz et al. 1987; Wang et al. 2005). More recently, in vivo studies where mice were inoculated by the intracerebral route with recombinant RABV mutants encoding a P protein able or not to decrease the type I IFN signaling revealed a good correlation between the severity of the disease and the capacity of the virus to escape the type I IFN response in the brain (Ito et al. 2010; Masatani et al. 2010a; Rieder et al. 2011). However, RABV contamination usually occurs after a bite resulting in an intramuscular inoculation. Thus, RABV has to pass through additional barriers mounted by the host innate defense such as mechanisms triggered at the site of inoculation and mechanisms in the spinal cord as described for Polio virus (Kuss et al. 2008; Pfeiffer 2010). In this study, we investigate the role of the type I IFN response on RABV infection in mice using a neuroinvasive viral strain causing fatal encephalitis after inoculation by the intramuscular route to mimic a natural way of infection. We chose to study RABV infection in two mouse models with targeted disruption of the IFNAR. The first mouse model ($IFNAR^{-/-}$) is a 129/Sv mouse lacking IFNAR expression in both the periphery and the NS (Muller et al. 1994). The second model is a C57BL6 NesCre ($^{+/-}$) IFNAR ($^{flox/flox}$) mouse lacking IFNAR only in neural cells of neuroectodermal origin (e.g., neurons, astrocytes, and oligodendrocytes) (Detje et al. 2009). Because IFNs regulate both innate and immune response acting directly or indirectly on most immune effectors (Trinchieri 2010), and prevents monocytes infiltration through the brain vessels (Floris et al. 2002; Prinz et al. 2008; Veldhuis et al. 2003), it cannot be excluded that immune responses in $IFNAR^{-/-}$ mice are decreased, making it difficult to sort out events controlled by IFN exerted in the NS from those controlled by IFN in the periphery. In contrast, this will not occur in the NesCre ($^{+/-}$) IFNAR ($^{flox/flox}$) mouse since the IFN response will be impaired in the NS only and not in the peripheral tissues. Therefore, the NesCre ($^{+/-}$) IFNAR ($^{flox/flox}$) mouse constitutes an appropriate model to study the role of IFN response in the RABV-infected NS.

We characterized the ability of the neuroinvasive RABV strain to trigger and counteract the type I IFN response in human neuronal cells. We studied the antiviral role of type I IFN on RABV infection by comparing infection in primary neuronal cultures (DRGs) of WT and IFNAR mice and by studying the effect of exogenous IFN-β treatment on RABV infection of human neuroblastoma cells. Then, we compared severity and kinetics of clinical signs, mortality, and progression of the infection in the NS of WT, $IFNR^{-/-}$, and NesCre ($^{+/-}$) IFNAR ($^{flox/flox}$) to define the role of the type I IFN response on RABV pathogenesis.

Results

The neuroinvasive RABV strain CVS-NIV counteracts the type I IFN response in human neuroblastoma cells by inhibiting IRF3 phosphorylation and STAT2 translocation

Most RABV strains, but may be not all of them (Ito et al. 2010; Masatani et al. 2010a; Shimizu et al. 2006), have the property to shut down type I IFN production by inhibiting the phosphorylation of IRF3/7 and to inhibit the type I IFN mediated transcription of ISGs by blocking the translocation of STAT-2/STAT-1 complex into the nucleus. Thus, at first we checked whether the neuroinvasive RABV CVS-NIV used in this study has the property to shut down type I IFN production and to inhibit the type I IFN signaling. Mock-infected (NI) human neuroblastoma SKNSH cells or 36 h-RABV-infected (MOI 3) SKNSH cells were treated with human IFN-β (500 IU/ml) for 6 h or left untreated (NT) (Fig. 1a), and co-labeled 6 h later with STAT2 and RABV P protein specific Abs and DAPI (nuclei marker) (Fig. 1b). In absence of infection, IFN-β treatment induces STAT2 translocation to the nucleus, whereas no such re-location was observed in RABV-infected cells. To check whether impaired STAT2 translocation also affects ISG transcription, the transcription of the ISG *2′–5′-oligoadenylate synthetase 1* (*OAS1*) gene was studied using qRT-PCRs in NI SKNSH and 36 h RABV-infected SKNSH treated with IFN-β (range from 0.5 IU to 500 IU/ml IFN-β) for 6 h (Fig. 1c). Compared to NI SKNSH, RABV-infected cells showed a 30-fold increase in *OAS1* transcription. This increase was 10-fold reduced when compared with NI cells treated for 6 h with IFN-β (200- to 600-fold increase when compared with NI, depending on the amount of IFN added to the cell culture). Exogenous IFN-β addition to RABV-infected cells does not enhance low *OAS-1* transcription of RABV-infected cells. This loss of reactivity is not due to IFN-β induced cell unresponsiveness but caused by viral infection since SKNSH treated with IFN-β is still reactive to a second IFN-β stimulation (supplementary data Fig. S1). In conclusion, these results indicate that RABV infection inhibits type I IFN signaling.

To test whether the CVS-NIV strain also interferes with type I IFN induction, we studied IRF3 phosphorylation in RABV-infected SKNSH cells and in SKNSH treated with poly I:C, a synthetic TLR3 ligand known to induce IRF3 phosphorylation, which is a mandatory step in IFN induction (Vercammen et al. 2008). IRF3 phosphorylation was analyzed in NI SKNSH either non-treated or treated with poly I:C and in RABV-infected SKNSK either non-treated or treated with poly I:C by Western blotting using an Ab targeting the Ser^{396} of IRF3 (Fig. 1d). Analyses were performed 15, 24, and 48 h after infection. Detection of RABV P protein was used as a control of infection, whereas tubulin served as a control of gel loading and TLR3 as a control protein which expression in SKNSH should not be altered upon RABV infection (Menager et al. 2009). In absence of infection, poly I:C treatment induced strong IRF3 phosphorylation, whereas IRF3 phosphorylation was almost undetectable in poly I:C treated RABV-infected cells. Furthermore, only faint IRF3 phosphorylation was detected in non-treated RABV-infected cells which showed up with delayed kinetics. These observations demonstrate that RABV CVS-NIV interferes with the type I IFN induction.

Altogether, our results indicate that as in most RABV strains, the neuroinvasive RABV strain CVS-NIV can inhibit both type I IFN induction and signaling.

Despite evasion of type I IFN, RABV infection still triggers type I IFN responses in neuronal cells and in the NS

Despite virus-mediated inhibition of type I IFN triggering and signaling, it can be noted that, compared with non-infected cells, RABV infection still triggers some *OAS-1* transcription and IRF3 phosphorylation (Fig. 1), suggesting that the RABV strategy to evade type I IFN induction is incomplete. To analyze further characteristics of residual type I IFN responses, we studied the kinetics of *IFN-β*, *ISG-20*, and *OAS-1* transcription in SKNSH infected with RABV at MOI 1 (Fig. 2a). The transcription of *IFN-β*, *ISG-20*, and *OAS-1* genes follows a bell-shaped induction with the maximum reached at 24 h pi indicating that RABV CVS-NIV triggers a transient type I IFN response. We noticed that the timing of the type I IFN response, but not the shape of the curve, was influenced by the MOI: the higher the MOI, the earlier the type I IFN response (data not shown). The induction of *IFN-β*, *ISG-20*, and *OAS-1* gene transcription does not result from a transitory infection of SKNSH since RABV N protein expression does not decrease but instead increases with time (Fig. 2a, left panel).

When WT mice were inoculated with RABV by an intramuscular route and were sacrificed at different stages of pathology (numbers with 1=animal with ruffled fur, 2=one paralyzed leg, 3=two paralyzed legs, and 4=moribund), a transient type I IFN response characterized by *IFN-β* and *OAS1* gene transcription was also observed in the spinal cord and brain of infected mice at early stages of the disease (Fig. 2b). Altogether, these observations indicate that the efficiency of the mechanisms selected by RABV to counteract the host type I IFN RABV suffers from some leakiness, allowing a residual type I IFN to settle in the early stages of infection, both in vitro and in vivo.

Role of the type I IFN signaling on RABV infection in primary cultures of DRGs

To figure out whether this residual and transient type I IFN induction modulates RABV infection, we compared at first

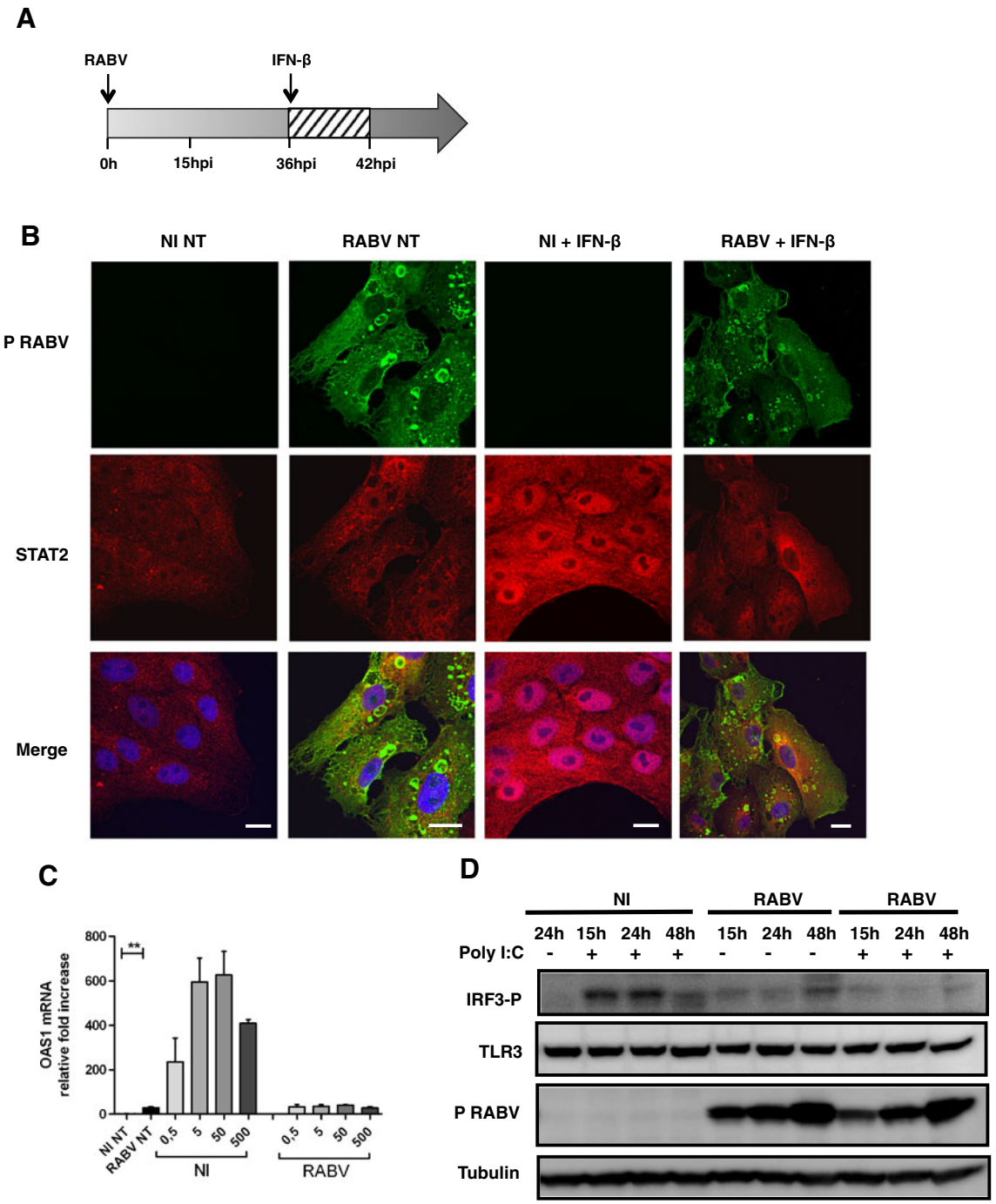

Fig. 1 RABV infection inhibits type I IFN signaling pathways. **a** SKNSH cells were infected with RABV (MOI 3) or mock-infected (NI) for 36 h, and then treated or not (NT) with IFN-β (500 IU/ml) for 6 h. **b** Six hours later (42 h pi), cells were immunostained for RABV P protein (*green*) and STAT2 (*red*) expression, counterstained with Dapi (nuclei in *blue*), and analyzed by confocal microscopy. *Scale bars* represent 10 μm. **c** NI or 36 h RABV-infected SKNSH were either NT or 6 h treated with different doses of IFN-β (0.5, 5, 50, or 500 IU/ml). Six hours later (42 h pi), RNAs were extracted and *OAS-1* gene transcription was compared by qRT-PCR in the different cultures. Results are expressed as relative fold increase of *OAS-1* mRNAs taking NI NT condition as a standard value of 1. They are presented as mean±standard errors of the means, SEM (**$p \leq 0.005$). **d** Detection by Western blotting of IRF-3 phosphorylation (Ser^{396}), TLR3, RABV P protein, and tubulin in 15, 24, and 48 h cultures of NI or RABV-infected SKNSH cells either NT or treated with poly I:C. Data are representative of at least two independent experiments

the RABV infection in primary neuronal cultures prepared from the dorsal root ganglia (DRG) of adult WT and IFNAR$^{-/-}$ mice (Fig. 3), and secondly we analyzed the effect of different IFN-β treatments (testing different timing and doses) on the infection of human neuroblastoma SKNSH cells (Figs. 4 and 5).

Primary cultures of DRG from adult WT and IFNR$^{-/-}$ mice were infected with RABV at a MOI 0.1. After 48 h of culture, WT and IFNAR$^{-/-}$ infected neurons were stained with FITC-conjugated Ab directed against RABV NC, and percentages of infected cells were calculated. As indicated in Fig. 3a, IFNAR$^{-/-}$ neurons showed a 2-fold enhanced infection than WT neurons (49% of infection in IFNAR$^{-/-}$ neurons compared to 27% in WT neurons). In addition, IFNAR$^{-/-}$ infected neurons seem to express higher viral proteins loads than those of WT cultures (Fig. 3b). The higher susceptibility of IFNAR$^{-/-}$ neurons compared to WT neurons and their higher viral protein content indicate that a functional IFNAR signaling protects neurons from infection and decreases viral multiplication, at least partially.

When the same cultures were infected with a higher MOI (MOI 1), the difference between IFNAR$^{-/-}$ and WT neurons declines (80% and 93% of infection in WT and IFNAR$^{-/-}$ DRGs cultures, respectively; Fig. 3c). This last observation suggests that the antiviral effect of IFN results from the triggering of a refractory state in non-infected neurons, a mechanism which cannot function anymore when all neurons are infected, a condition occurring when cultures are infected with a MOI of 1.

These data highlight that the transient type I IFN response triggered during RABV infection is not neutral and instead can reduce infection, likely by triggering both a refractory state in some cells and by diminishing the protein viral load in infected cells.

To further study these mechanisms of action, we first analyzed the effect on RABV infection of SKNSH treated with 5.0 IU/ml of IFN-β given for 6 h prior to RABV infection (Fig. 4a).

When RABV transcription was analyzed by qRT-PCR in non-treated SKNSH (−IFN) and in IFN-β treated (+IFN)

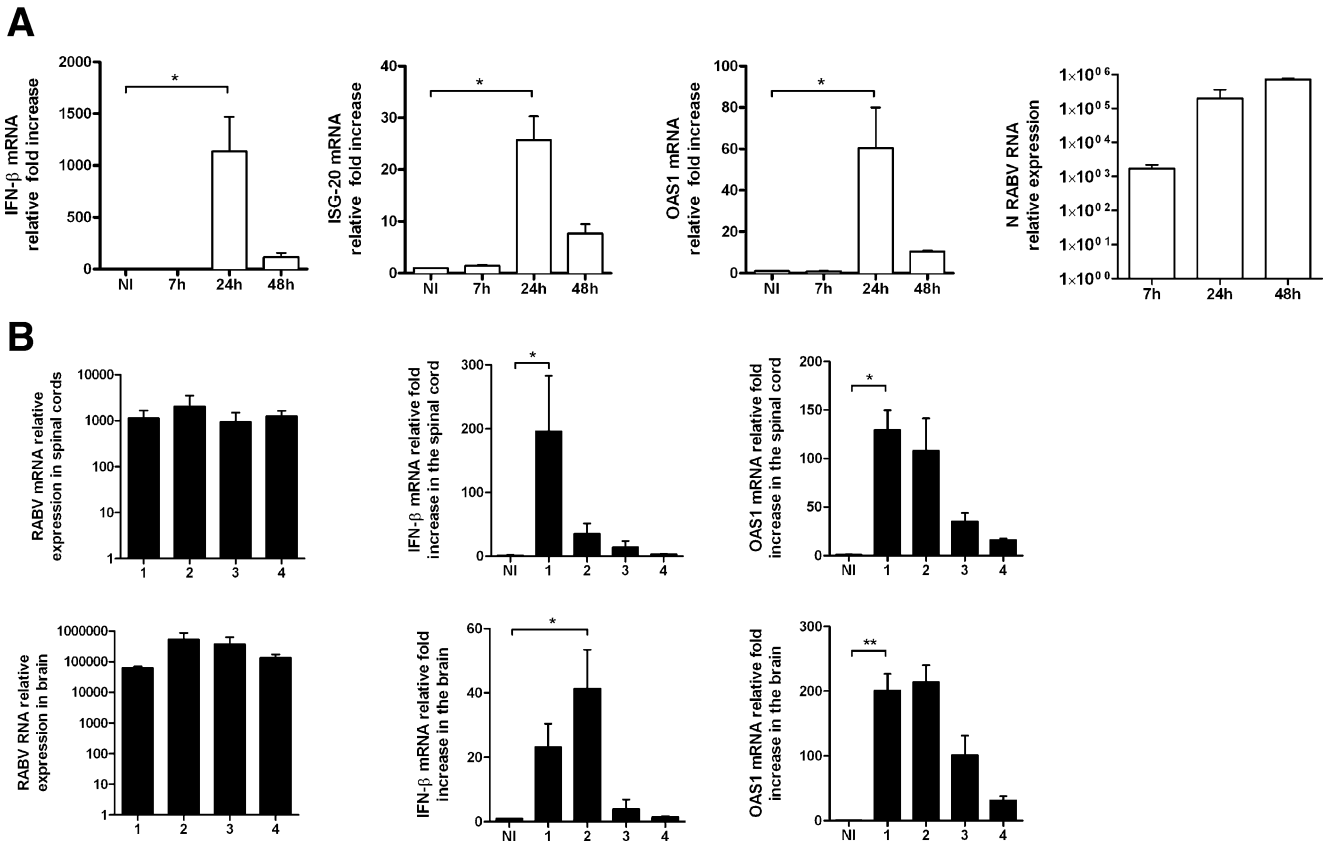

Fig. 2 Despite evasive strategy, RABV triggers a type I IFN response that slows down RABV infection both in vitro and in vivo. **a** Human neuroblastoma SKNSH cells were infected (MOI 1) with CVS-NIV for 7, 24, and 48 h. Transcription of *IFN-β* (*left panel*), *ISG-20* (*middle left panel*), *OAS-1* (*middle right panel*), and of RABV *N protein* was analyzed by qRT-PCR. Data are representative of at least two independent experiments and are presented as mean±SEM (*$p \leq$ 0.05). **b** WT mice (6-week-old female C57BL6 mice) were infected i.m. with CVS-NIV. Mice were sacrificed at different stages of infection (1–4), perfused with saline buffer, and spinal cord and brain were removed. Transcription of *N protein*, *IFN-β*, and *OAS-1* was determined by qRT-PCR in spinal cord and brain. Experiments were performed at least three times. Each group consists of two to three animals. Data are presented as mean±SEM (**$p \leq 0.005$, *$p < 0.05$)

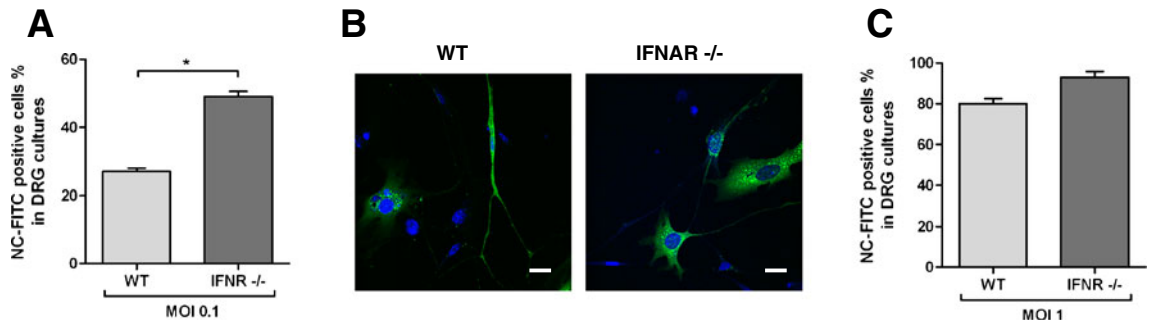

Fig. 3 Role of type I IFN on RABV infection in cultures of primary mouse neurons dorsal root ganglia (*DRG*) neurons from WT and IFNAR$^{-/-}$ mice were infected with RABV at a MOI 0.1 (**a**) or MOI 1 (**c**) and stained 48 h pi with Ab directed against RABV NC (**a** and **c**) or P protein (**b**). Percentage of infected cells (NC-FITC positive cells) was determined by counting at least 200 cells in each type of cultures. Data are presented as mean±SEM (*p<0.05)

SKNSH, it appears that the pre-treatment of SKNSH with IFN drastically reduces, but does not abrogate (drop of 56% 15hpi), the virus transcription. This effect is a long-lasting effect, still present 40 h after infection (Fig. 4b). When cells

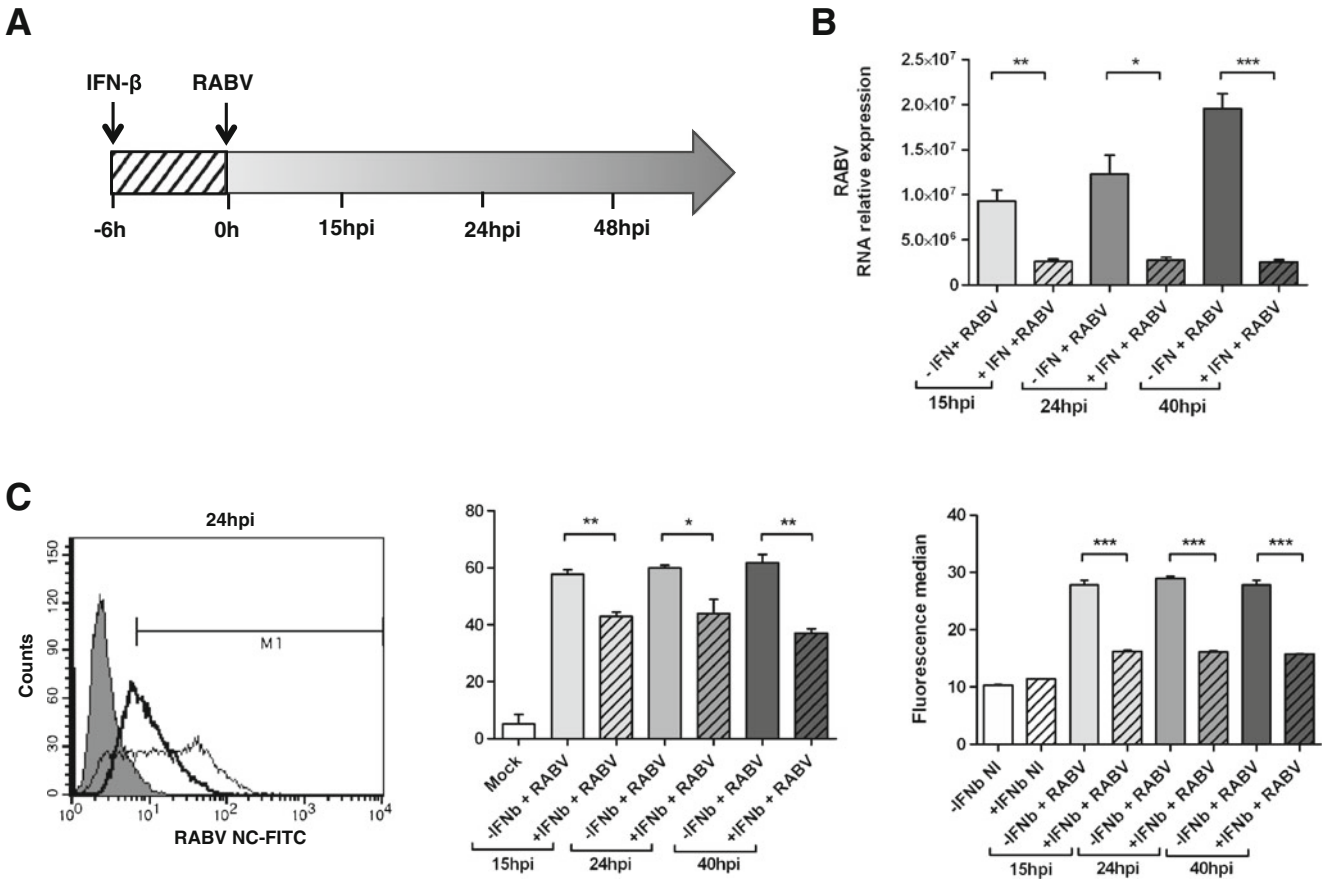

Fig. 4 Type I IFN given before infection triggers a refractory state and in human neuroblastoma SKNSH. SKNSH cells treated—or not treated—with IFN-β (5.0 IU/ml) for 6 h pre-RABV infection and collected 15, 24, and 48 h pi to perform or qRT-PCR and flow cytometry. **a** Scheme of treatment. **b** qRT-PCR targeting RABV *N protein* gene were made on IFN-β treated (+IFN) and non-treated cells (−IFN) for 6 h with IFN-β (5.0 IU/ml) prior to RABV infection at 15, 24, or 40 h pi to measure RABV transcription. **c** RABV NC expression was monitored 24 h pi using flow cytometry. In the *left panel*, the number of cells expressing different fluorescence intensities were compared between RABV infected mock-treated cells (*black thin line*), RABV-infected cells treated for 6 h before the infection (5.0 IU/ml) (*black bold line*), and NI mock-treated cells (*gray fill curve*). M1 is the gate in which cells are considered as positive for NC expression. *Middle panel* plots the kinetic of infected cells (percentage of cells present in M1) according to the treatment applied to the cultures. *Right panel* represents the kinetic of accumulation of viral NC in the M1 according to the treatment they received (median of fluorescence in M1). Data are presented as mean±SEM (***p<0.0005, **p≤0.005, *p<0.05)

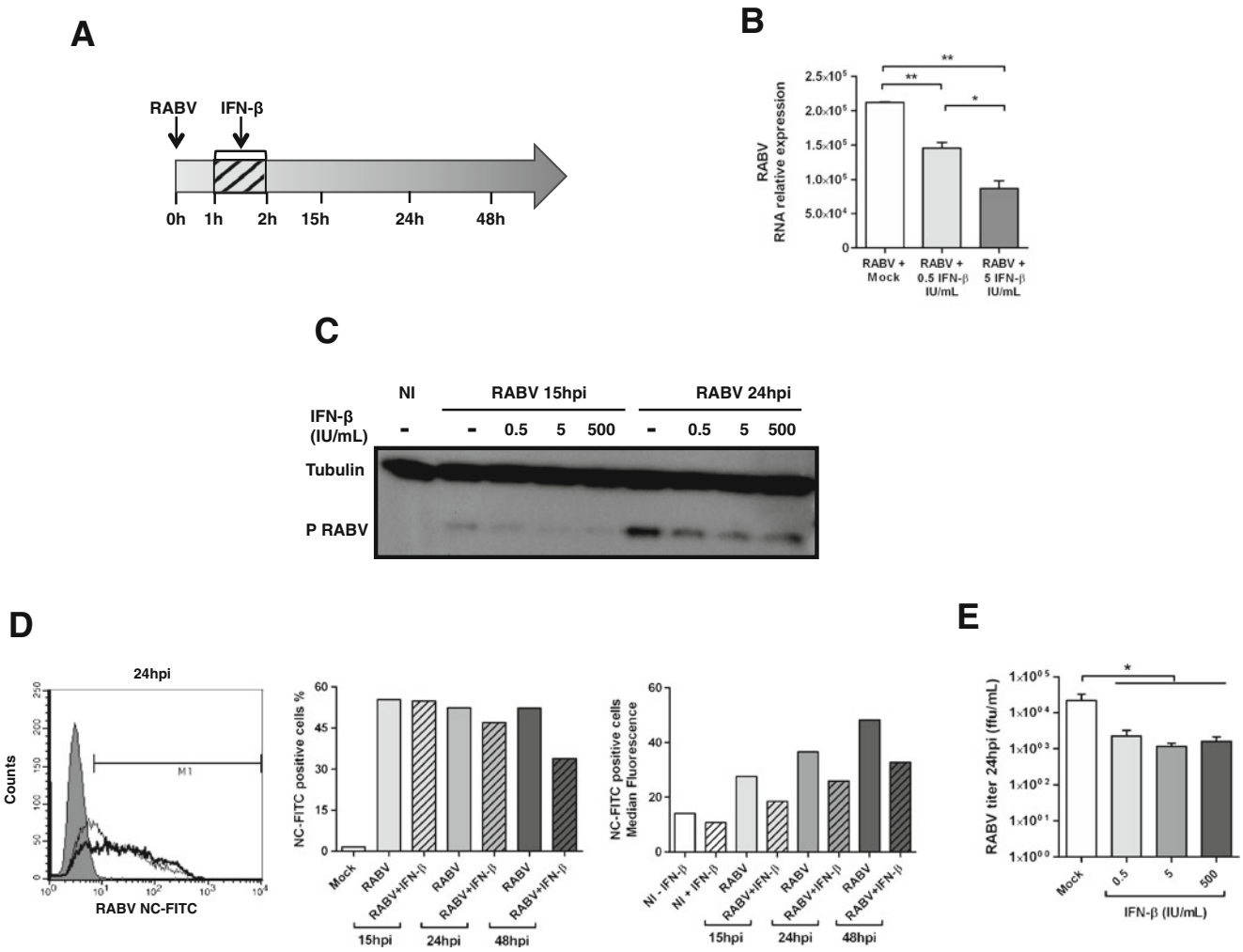

Fig. 5 Type I IFN given after the infection does not prevent infection but limits RABV multiplication. **a** Scheme of IFN treatment. **b** RABV transcription was determined in non-treated and IFN treated cultures (0.5 and 5.0 IFN-β IU/ml) using qRT-PCR 24 h pi for *N protein* transcription. **c** Expression of RABV P protein was compared by Western blotting using P protein specific mAb in either NI, or RABV-infected cells treated with 0.5, 5.0, or 500 IU/ml or non-treated (−) at two times pi (15 h and 24 h). Tubulin is used a control for gel loading. **d** 24 h pi RABV NC expression was monitored using flow cytometry in RABV-infected mock-treated cells (*black thin line*), RABV-infected cells treated for 1 h after the infection (0.5 IU/ml) (*black bold line*), and in NI mock-treated cells (*gray fill curve*). M1 is the gate which defines NC-FITC positive cells. *Middle* and *left panels* represent percentage of infected cells (M1%) and expression of NC protein (mean fluorescence in M1). **e** Viral progeny was determined as ffu/ml in the supernatants of 24 h RABV-infected cultures either mock-treated or treated with 0.5, 5.0, or 500 IU/ml. Data are presented as mean±SEM (**$p \leq 0.005$, *$p < 0.05$)

were stained with a FITC-conjugated Ab specific for RABV NC and the infection of the cultures was monitored by flow cytometry (Fig. 4c), it appears that the pre-treatment of SKNSH with IFN slightly reduces the percentage of infected cells (a 15% decrease with 60% of infection in non-treated versus 40% in treated cultures). In the meantime, the amount of viral NC was reduced by 2-fold (a mean fluorescence of 30 in non-treated compared to a mean fluorescence of 15 in treated cells).

Altogether, these data indicate that a pre-treatment with IFN-β does trigger a refractory state, but in only a fraction of the population, and has a significant impact on RABV protein (NC) expression.

Then, to evaluate the potential effect of a transient pulse of type I IFN on RABV infection, SKNSH were treated with type I IFN for 1 h after being infected (Fig. 5a). RABV transcription, protein expression, and virus production were studied in treated and non-treated conditions.

After 24 h infection, RABV *N protein* transcription is decreased by 31% and 58% when cells were treated for 1 h with respectively 0.5 IU/ml and 5.0 IU/ml of IFN-β (Fig. 5b). This result indicates that transient exposure to type I IFN can slow down RABV transcription in a dose-dependent manner. The effect of IFN-β treatment on transcription is associated to a decrease in protein expression as illustrated for P protein (Western blotting in Fig. 5c).

The lower P protein expression in IFN-β treated cells compared to non-treated cells at 15 and 24 h pi indicated that a transient IFN-β stimulation decreases RABV viral P protein expression. To figure out whether this lower expression of viral protein was due to a decrease of the number of infected cells or an intrinsic decrease of protein expression, percentage and mean fluorescence in infected cultures treated or not treated for 1 h with 0.5 IU/ml of IFN-β were analyzed by flow cytometry as described above (Fig. 5d). Percentage of RABV-infected cells were similar in IFN-β treated and non-treated cultures at earlier stages of infection (15 and 24 h pi), whereas percentage of infected cells in IFN-β treated cultures were one third lower than in non-treated cells at later stages of infection (48 h pi). RABV NC mean fluorescence was reduced in IFN-β treated cells compared to non-treated but was not blocked since it still increases with time, as observed for non-treated cells.

Altogether, these observations indicate that after RABV infection, transient exposure of already infected cells to low dose of type I IFN decreases RABV protein expression. Similar conclusions were made when cells were treated with a higher dose (500 IU/ml) of type I IFN (supplementary data in Fig. S2).

Production of RABV infectious particles was assayed in the supernatants of RABV-infected SKNSH either non-treated or treated with a 1 h pulse of IFN-β. As shown in Fig. 5e, the IFN treatment reduces viral production by 1 log in a dose-independent manner. This observation indicates that a transient treatment of infected cells with type I IFN is sufficient to reduce viral progeny.

Type I IFN signaling deficiency promotes RABV dissemination in muscles and facilitates RABV accessibility to the brain

Since stimulation of the type I IFN response is able to reduce RABV infection, we investigate whether the type I IFN response triggered during RABV infection modulates RABV neuroinvasiveness in vivo.

To mimic a classical way of infection, we inoculated WT and IFNR$^{-/-}$ mice in the thigh muscles of both hind limbs with RABV and we collected the inoculated muscles 2, 4, and 7 days pi to determine by qRT-PCR both *OAS1* and *N protein* gene transcription at the inoculated site (Fig. 6a).

Transcription of *OAS1* gene, used as a marker of the type I IFN response, was induced in the muscle of RABV-infected WT mice as early as 2 days pi (Fig. 6a, left panel). Transcription of *OAS-1* gene doubles between day 2 and day 4 pi and again between day 4 and day 7 pi in the muscles of RABV-infected WT mice, while as expected the *OAS-1* transcription was not detected in the muscle of RABV-infected IFNR$^{-/-}$ mice. RABV *N protein* transcription, used as a marker of RABV multiplication, was significantly higher (by at least 10-fold) in the muscles of RABV-infected IFNAR$^{-/-}$ mice compared to those of RABV-infected WT mice. These results indicate that after an intramuscular inoculation, RABV launches a type I IFN response with antiviral property able to limit RABV multiplication in the inoculated muscles.

Type I IFN response in the NS reduces RABV pathogenicity by delaying neuroinvasiveness

To test the specific effect of the type I IFN response in the CNS on RABV infection, 129/S2/Sv WT and IFNAR$^{-/-}$ mice were intramuscularly inoculated with RABV and sacrificed 2, 4, and 7 days pi to measure RABV *N protein* transcription in their brains and spinal cords (Fig. 6b). The increase of RABV *N protein* transcription observed in the muscle of IFNAR$^{-/-}$ mice was accompanied by an earlier (day 2 pi) detection of viral transcripts in the spinal cord of IFNAR$^{-/-}$ mice compared to WT mice, with a 100-fold increase (Fig. 6, left panel). However, the difference disappeared by day 4 and thereafter. In contrast, no differences were seen in the brain infection at any time (Fig. 6, right panel). C57Bl6 WT and NesCre ($^{+/-}$) IFNAR ($^{flox/flox}$) mice were intramuscularly inoculated with RABV and sacrificed 5 and 7 days pi. RABV *N protein* transcription was higher in the spinal cords of NesCre ($^{+/-}$) IFNAR ($^{flox/flox}$) mice 5 days pi compared to WT mice, with a 100,000-fold increase in the spinal cord of NesCre ($^{+/-}$) IFNAR ($^{flox/flox}$) mice compared to C57BL6 WT mice (Fig. 6c, left panel). RABV *N protein* was actively transcribed in the brain of NesCre ($^{+/-}$) IFNAR ($^{flox/flox}$) mice as soon as 5 days pi, whereas RABV *N protein* transcription could not be detected that early in the brain of RABV-infected C57BL6 WT mice (Fig. 6c, right panel). In contrast, after 7 days of infection, the difference of viral transcription between C57BL6 WT and NesCre ($^{+/-}$) IFNAR ($^{flox/flox}$) vanished, with similar RABV *N protein* mRNA levels in C57BL6 WT and NesCre ($^{+/-}$) IFNAR ($^{flox/flox}$) both in the spinal cord and brain.

The disappearance of the antiviral effect at later stages of infection [day 4 pi for IFNARs and day 7 pi for NesCre ($^{+/-}$) IFNAR ($^{flox/flox}$) mice] reminds us of the observation made with DRGs (Fig. 3) in which the antiviral effect is not seen any more when all cells in culture are infected (MOI 1), a condition which does not allow the refractory state to set up anymore.

Altogether, these results indicate that after intramuscular inoculation, the IFN response triggered by RABV in the CNS efficiently delays the infection of the nervous tissues at the early stages of infection, but this antiviral effect is inefficient at later stages of infection.

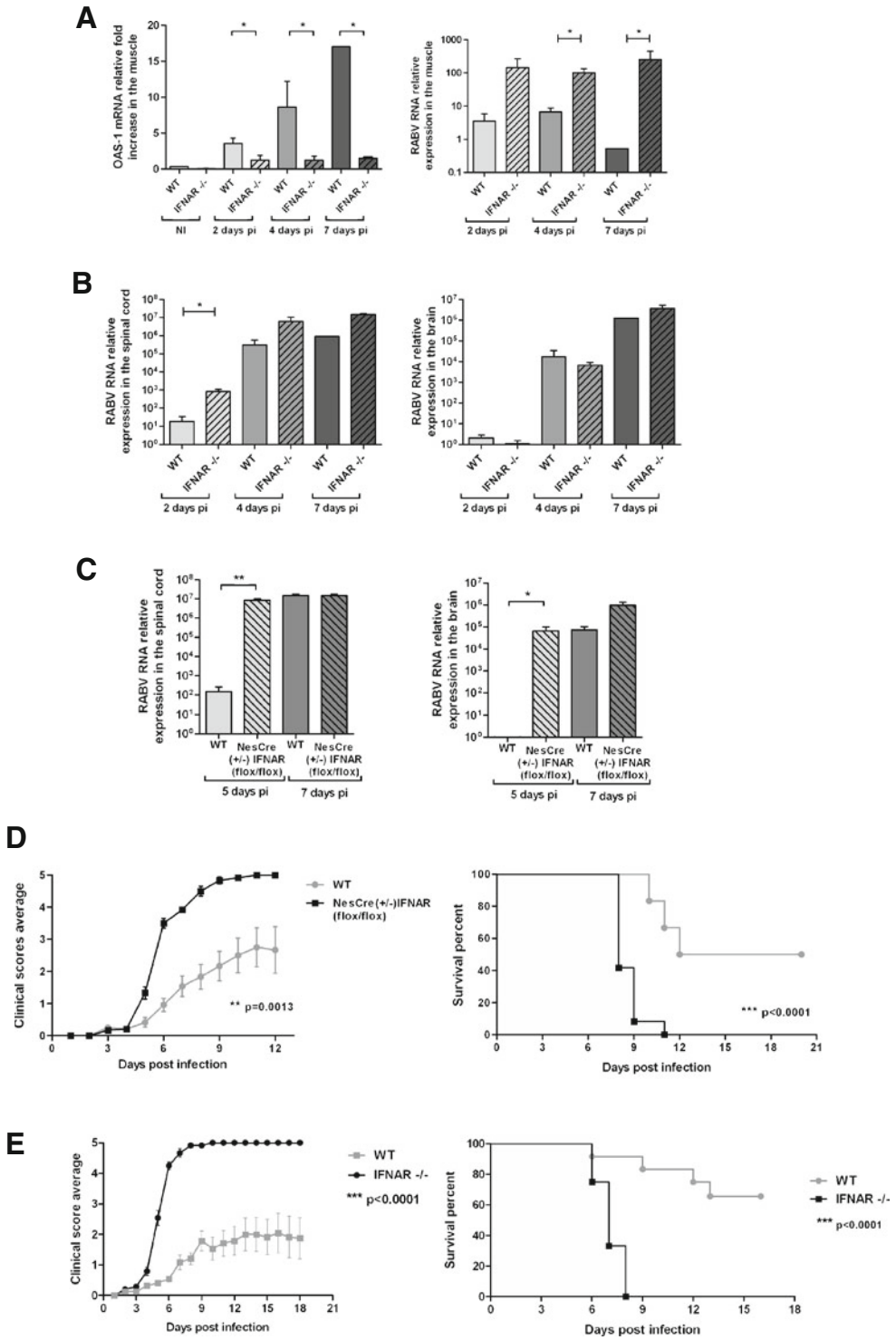

Fig. 6 The type I IFN response limits RABV dissemination in the inoculated muscle and slows down RABV infection in the NS. **a** WT (129/S2/Sv) and IFNR$^{-/-}$ mice were sacrificed 2, 4, or 7 days post-hind legs i.m. inoculation of RABV, and intracardially perfused. Thigh muscles, spinal cords, and brain were sampled. Transcription of *OAS1* gene (*left panel*) and RABV *N protein* gene (*right panel*) was determined in muscles using qRT-PCR (n=4) (*p<0.05). **b** RABV *N protein* gene transcription was compared by qRT-PCR in spinals cords (*left panel*) and brains (*right panel*) of 129/S2/Sv WT and IFNAR$^{-/-}$ mice 2, 4, and 7 days post i.m. inoculation with RABV (n=3). Data are presented as mean±SEM (*$p\leq$0.05). **c** WT (C57BL6) and NesCre ($^{+/-}$) IFNAR ($^{flox/flox}$) mice were sacrificed 5 or 7 days post-hind legs i.m. inoculation of RABV, and intracardially perfused. Spinal cords and brains were sampled. RABV *N protein* gene transcription was compared by qRT-PCR in spinals cords (*left panel*) and brains (*right panel*) (n=3). Data are presented as mean±SEM (*$p\leq$0.05; **$p\leq$0.005). **d** Pathogenicity was compared between C57BL6 WT mice and NesCre ($^{+/-}$) IFNAR ($^{flox/flox}$) mice by monitoring clinical scores (*left panel*) and survival rate (*right panel*) (n=12 per group). **e** Pathogenicity was compared between 129/S2/Sv WT mice and IFNAR$^{-/-}$ mice by monitoring clinical scores (*left panel*) and survival rate (*right panel*) (n=12 per group)

The effect of the type I IFN response in the CNS on RABV pathogenesis was assayed by monitoring clinical scores and survival of C57BL6 WT and NesCre ($^{+/-}$) IFNAR ($^{flox/flox}$) mice and of 129/S2/Sv WT and IFNAR$^{-/-}$ mice (Fig. 6d, e). Although the first sickness signs (ruffled fur, weakness) appear at the same time around 5 days pi in both WT and NesCre ($^{+/-}$) IFNAR ($^{flox/flox}$) mice, CNS specific type I IFN deficiency leads to more rapid progression of the clinical signs to severe disease in NesCre ($^{+/-}$) IFNAR ($^{flox/flox}$) mice compared to C57BL6 WT mice. The accelerated progression of the pathology in NesCre ($^{+/-}$) IFNAR ($^{flox/flox}$) mice correlates with earlier death in NesCre ($^{+/-}$) IFNAR ($^{flox/flox}$) mice than in C57BL6 WT mice, with 50% of the NesCre ($^{+/-}$) IFNAR ($^{flox/flox}$) mice being dead 8 days pi, whereas this score was reached by C57BL6 WT mice 12 days pi and higher mortality rate was reached in NesCre ($^{+/-}$) IFNAR ($^{flox/flox}$) mice than in WT mice [RABV causes death in 100% of NesCre ($^{+/-}$) IFNAR ($^{flox/flox}$) and in only 50% of WT mice]. Similar observations were made when CVS-NIV pathogenicity was compared between RABV-infected 129/S2/Sv WT and IFNAR$^{-/-}$ mice (Fig. 6e) with clinical signs starting in WT and IFNAR$^{-/-}$ mice 4 days pi and all IFNAR$^{-/-}$ mice being dead at day 11 pi.

Altogether, these data indicate that type I IFN deficiency in the NS accelerates RABV pathogenesis, precipitates death, and doubles the number of casualties. Altogether, these data indicate that type I IFN which is still produced in the NS during RABV infection is efficient enough to reduce neuroinvasiveness and pathogenesis and partially protect the infected host from fatal infection.

Discussion

RABV virulence relies on several factors: among others, RABV infection triggers survival of infected neurons (Prehaud et al. 2010) and RABV escapes adaptive immunity (Baloul et al. 2004; Galelli et al. 2000; Lafon 2008; Lafon et al. 2008). The ability of RABV to dampen the host innate immune response has been suspected to be an additional arm of the evasion strategy of RABV (Chopy et al. 2011; Wang et al. 2005). Here, we investigated the role of the type I IFN response on RABV infection both in vitro and in vivo, using a RABV strain causing fatal encephalitis after an intramuscular injection into the hind limb—a route mimicking a natural infection—and two mouse models lacking IFNAR: conventional IFNAR$^{-/-}$ and the newly described NesCre ($^{+/-}$) IFNAR ($^{flox/flox}$) mouse with a deficiency of IFNR restricted to the CNS (Detje et al. 2009).

We observed in IFNAR deficient DRGs that RABV infection was increased. Treatment with low doses of type I IFN before RABV infection decreased RABV infection of neuronal cells. When exogenous IFN-β was given after infection, the antiviral effect of IFN-β was dependent on the amount and on the timing with which IFN was added to the already infected cultures. In vivo, RABV accessibility to the CNS was faster in absence of IFNAR, leading to earlier death with a much higher death toll in IFNAR deficient mice than in WT mice. Altogether, the in vitro and in vivo data consistently demonstrated that RABV infection is indeed sensitive to the antiviral effect of type I IFN response. This confirms previous observations made by Faul and colleagues with recombinant RABV expressing type I IFN whose replication was greatly reduced (Faul et al. 2008).

We showed that the neuroinvasive RABV strain (CVS-NIV) used in this study has developed strategies to counteract type I IFN triggering and signaling, similar to those strategies already described for other RABV strains (Brzozka et al. 2005; Masatani et al. 2010b; Vidy et al. 2005). Indeed, the RABV CVS-NIV inhibits IRF3 phosphorylation and blocks STAT2 translocation to the nucleus. By these mechanisms, RABV blocks not only the production of IFN but also the usage of IFN by cells in a paracrine or autocrine manner. Despite these efficient mechanisms to grid-lock the type I IFN system, a transient IFN-β was still induced in the infected cells at the early stage of infection. This pulse of IFN-β transcription was followed by secretion of IFN-β into the supernatant of the infected cultures (Prehaud et al. 2005). Moreover, in the brain of infected mice, *IFN-β* transcription was observed at the early stages of infection when mice showed first mild clinical signs, whereas *IFN-β* transcription declined as the clinical signs and infection worsened. Altogether, these data indicate that the strategy of the virus to counteract the type I IFN response is leaky, leading to the production of type I IFN in the infected CNS. In addition to the residual IFN-β produced by the infected neurons at the early stages of the infection, IFN-β can also be produced in the infected CNS by non-infected glial cells because these cells do not express the viral proteins known to downregulate the IFN response. This heterocellular IFN which has been shown to be functional in other viral models (Chen et al. 2010) may also contribute to the production of IFN in the infected NS despite the counteracting strategy set up by RABV.

One can wonder what the role of the residual IFN-β expression on RABV infection is and ask whether such leakiness impacts RABV infection. Comparison of RABV pathogenicity in WT and NesCre ($^{+/-}$) IFNAR ($^{flox/flox}$) mice indicates that residual IFN production is efficient enough to bridle neuroinvasiveness and partially protect the host against fatal infection. Besides, it can be thought that the residual type I IFN has the capacity to prevent infection of the neighboring cells. Indeed, in contrast to WT mice, an intramuscular inoculation of RABV in IFNAR$^{-/-}$ mice

resulted in the infection of the muscle suggesting that the type I IFN response might indeed curtail dissemination of RABV in the peripheral tissues. This result reminds us of previous reports in other infections showing that type I IFN host responses promote the neurotropism of Polio virus (Ida-Hosonuma et al. 2005; Kuss et al. 2008; Pfeiffer 2010) and of other pathogens (Conrady et al. 2010; Fragkoudis et al. 2009; Ireland et al. 2008; McFadden et al. 2009) by limiting targeting and spreading in non-neuronal cells. In RABV infection, this restriction might have no effect on the already infected neurons since we showed that an exogenous IFN-β treatment of the already infected neurons cannot reverse the interference exerted by the virus on the IFN response. In contrast, a residual IFN production in the NS might favor the neuronotropism of RABV by avoiding the infection of glial cells. Alternatively, the pulse of IFN-β produced by the infected neurons could stimulate IFN-dependent genes such as B7-H1, a protein shown to be expressed into the RABV-infected brain and to favor RABV infection (Chopy et al. 2011; Lafon et al. 2008). Such a role of IFN in RABV pathogenesis will deserve further study.

Mice lacking IFNAR are highly susceptible to several viral infections (Conrady et al. 2010; Fragkoudis et al. 2009; Ireland et al. 2008; Muller et al. 1994; Steinhoff et al. 1995) with virus replicating to higher levels and mice dying two to three times faster than WT mice. RABV follows this pattern and IFNAR$^{-/-}$ and NesCre ($^{+/-}$) IFNAR ($^{flox/flox}$) mice were more rapidly infected by RABV and died faster than WT mice. The mechanism leading to the death of the RABV-infected host is still unclear (Jackson et al. 2008; Prehaud et al. 2010; Scott et al. 2008). Because NesCre ($^{+/-}$) IFNAR ($^{flox/flox}$) mice show an earlier death phenomenon compared to that observed in WT mice, they could be a helpful model to start investigating this point. When the kinetics of RABV transcription was studied in the CNS of WT and NesCre ($^{+/-}$) IFNAR ($^{flox/flox}$) mice, it appears that viral transcription occurs earlier in the spinal cord and in brain of NesCre ($^{+/-}$) IFNAR ($^{flox/flox}$) mice than in those of WT, whereas at later time points viral transcription was similar in the spinal cord and brain of both types of mice. Similar observations were made with IFNAR$^{-/-}$ mice in which the earlier death was linked to an earlier spinal cord invasion compared to WT mice. This suggests that early death of IFNAR is linked to the early invasiveness of their NS and confirms a previous observation made in our laboratory when the neuroinvasiveness of two RABV strains, CVS and PV, were compared in WT mice: we found that CVS, the strain causing fatal encephalitis, invades the spinal cord earlier (2 days) than PV, the strain causing abortive rabies only with no fatal casualties (Baloul et al. 2004). Thus, the speed with which RABV infects the spinal cord could be critical for the fatal outcome caused by this virus. These observations cast the idea that early multiplication or entry in the spinal cord is an IFN-dependent bottleneck controlling RABV pathogenicity. The size of the viral inoculum could also modulate the virus neuroinvasiveness since IFNAR$^{-/-}$ mice, in which the RABV transcription in the inoculated muscle was higher compared to WT mice, died earlier (6–9 days pi) than NesCre ($^{+/-}$) IFNAR ($^{flox/flox}$) mice (8–11 days pi) in which we assumed that RABV does not multiply in the muscle. This assumption was supported by the observation that NesCre ($^{+/-}$) IFNAR ($^{flox/flox}$) mice control a viral infection (the rabdovirus VSV) in the periphery as efficiently as WT mice do (Detje et al. 2009), a feature consistent with the fact that the IFN response in the periphery is not impeded in NesCre ($^{+/-}$) IFNAR ($^{flox/flox}$) mice. However, it may be inappropriate to compare the kinetic of death in IFNAR$^{-/-}$ and NesCre ($^{+/-}$) IFNAR ($^{flox/flox}$) mice since the two types of mice do not have the same genetic background. To note and as already reported in other viral infections (Raaben et al. 2009), susceptibility of 129/S2/Sv to RABV was reduced (25% mortality) compared to C57BL6 mice (50% mortality), making difficult the comparison of RABV infection in IFNAR$^{-/-}$ and NesCre ($^{+/-}$) IFNAR ($^{flox/flox}$) mice.

Exact mechanisms causing the death of the rabid animals are not well understood; it has been proposed that some may be related to neuronal exhaustion and hormonal deregulation (Fu and Jackson 2005; Scott et al. 2008; Torres-Anjel et al. 1988). It is not excluded that other factors such as the setting up of a pro-inflammatory neuronal environment may also contribute to lethality (Laothamatas et al. 2008; Wang et al. 2005; Zhao et al. 2009). A quicker viral invasion of the NS of IFNARs mice compared to WT mice may result in an exposure to lethal conditions long and strong enough to cause the premature death of the NesCre ($^{+/-}$) IFNAR ($^{flox/flox}$) and IFNAR$^{-/-}$ mice.

Although RABV has developed an efficient strategy to counteract type I IFN response, a type I IFN response is still triggered at the early stage of RABV infection suggesting that interference in type I IFN response is leaky. On one hand, this residual type I IFN, even if it cannot protect against the fatal outcome, can reduce RABV multiplication and slow down RABV progression into the NS leading to the conclusion that host survival may benefit from the residual type I IFN response. On the other hand, the IFN response can also favor the RABV neuronotropism by curtailing infection in muscle and possibly in glial cells, and also by up-regulating IFN-dependent molecules involved in RABV immunoevasive strategy such as B7-H1. In this case, type I IFN could be deleterious for the host survival. Thus, at this stage of our knowledge, it would be premature to recommend the use of IFN type or adjuvant compounds stimulating the host innate immune response as additional therapy to current rabies post-exposure treatment.

Material and methods

Cells and virus

Dorsal root ganglia (DRGs) and human neuroblastoma cells SKNSH (ATCC HTB11) were prepared and grown as previously described (Castellanos et al. 2005; Lafon et al. 2005). The laboratory RABV strain CVS (CVS-NIV), a highly pathogenic strain causing fatal encephalomyelitis in mice after intramuscular injection (Camelo et al. 2000), was propagated as previously described (Thoulouze et al. 1997). Cells were infected at a multiplicity of infection of 3 (MOI 3) and cultivated at 37°C in 5% CO_2. RABV infection was followed up by measuring *N protein* expression by qRT-PCR, P protein expression by Western blotting, and intracellular accumulation of NC by flow cytometry or confocal UV microscopy. Viral progeny was measured by testing a series of diluted cell culture supernatants on RABV susceptible monolayer cells and by detecting the fluorescent foci by microscopy.

Antibodies and reagents

Antibodies (Ab) were acquired as follows: FITC-conjugated rabbit anti-RABV NC (RABV NC-FITC) Ab from Bio-Rad; mouse polyclonal anti-tubulin from Oncogene Research; mouse anti-RABV P protein Ab (721.2) was a gift from Dr. T.J. Wiktor (Lafon and Wiktor 1985); mouse anti-STAT2 (C-20 sc-476) Ab from Santa Cruz Biotechnology; rabbit polyclonal anti-phosphorylated-STAT2 (Tyr689) Ab from R&D System; rabbit anti-phosphorylated-IRF3 (Ser396) Ab and rabbit anti-phosphorylated-STAT3 (Tyr705) Ab from Cell Signaling Technology; rabbit TrueBlot and Horseradish Peroxidase-conjugated anti-rabbit IgG was from eBioscience; and peroxidase-conjugated AffiniPure $F(ab')^2$ fragment donkey anti-mouse IgG was purchased from Jackson ImmunoResearch Laboratories. Poly I:C (heated at 50°C to increase the solubility) was obtained from InvivoGen and recombinant human IFN-β (Betaferon) was from Schering. CellFIX™ was from BD Biosciences. SuperSignal West Pico chemiluminescent was from Thermo Scientific. SuperScript II Reverse transcriptase was from Invitrogen. RNeasy and Qiazol kits were from Qiagene. Anti-protease and anti-phosphatase cocktails were from Roche. RIPA1 buffer was from Sigma. GoTaq qPCR Master Mix was from Promega.

Flow cytometry

Trypsinized cells were washed with $Ca^{2+}Mg^{2+}$ saline phosphate buffer (SPB) and fixed with paraformaldehyde 4%, 20 min at 4°C. After washing, cells were incubated for 30 min at 37°C with a FITC-conjugated rabbit polyclonal AB directed against RABV NC diluted (1/50) in permeabilization buffer (SPB, 1.0% FCS, 0.1% sodium azide, 0.1% saponine, pH 7.4). After final washes, cells were resuspended in CellFIX™ and analyzed using a BD Biosciences FACSCalibur equipped with Cell Quest Pro software. Ten thousand viable cells were acquired per sample. Analysis was performed on histogram plotting intensity of fluorescence emitted in the FL1 channel and numbers of cells. Results were presented as percentages of cells emitting in the FL1 channel with an intensity >10 and as mean of fluorescence expressed by these cells.

Western blotting and immunocytochemistry

For Western blotting, RABV- and mock-infected cells were lysed with RIPA buffer supplemented with anti-protease and anti-phosphatase cocktails and stored at −20°C. After denaturation, proteins (25 μg) were loaded onto a 4–12% Tris–Bis SDS NuPage gel (Invitrogen) with Kaleidoscope pre-stained standards (Bio-Rad). After transfer, PVDF membranes (Hybond-P; GE HealthCare) were saturated for 1 h at room temperature in saturating buffer (SPB–0.1% Tween and 5% bovine serum albumin). Membranes were incubated with primary Ab overnight at 4°C, washed four times in SPB–0.1% Tween, then incubated with secondary Ab coupled to horseradish peroxidase (1 h at room temperature). After washing, membranes were incubated in SuperSignal West Pico. To detect phosphorylated proteins, SPB was replaced by STB for incubation and washes. Signals were acquired with a GBOX monitored by the Gene Snap (Syngene) software. Band quantification was normalized on tubulin signal and expressed in fold increase based on control conditions (non-infected and non-treated cells or mice).

For immunocytochemistry, RABV- and mock-infected cells were stained and analyzed in UV microscopy as previously described (Menager et al. 2009).

RNA extraction, RT, and qPCR

Total RNAs were extracted with the RNeasy kit for cells or with Qiazol and the RNeasy kit for tissues. RNA quantity and quality were monitored using spectrophotometry (NanoDrop). cDNA synthesis was performed from 1 μg RNA using SuperScript II Reverse transcriptase with oligo dT primers. Real-time PCR (qRT-PCR) was performed in duplicate using the ABI PRISM 7500 Fast Sequence Detector system (Applied Biosystems) with the GoTaq qPCR Master Mix. After normalization to 18S RNA (used as a housekeeping gene), the relative abundance of mRNA was obtained by calculating the difference in threshold

cycles of the test and control samples (wild type, mock-treated, or non-infected cells or tissue, value set to 1), commonly known as the ΔΔCT method. RABV RNA quantification was normalized to 18S and a standard control. Sequences or references of primers used for RT-PCR are listed in Prehaud et al. (2005) or were purchased from QIAGEN.

Mice

Female C57BL/6J mice (Janvier, France), 129/S2/Sv (Charles Rivers, France), IFNAR$^{-/-}$ (Muller et al. 1994), and NesCre ($^{+/-}$) IFNAR ($^{flox/flox}$) (Detje et al. 2009) 6- to 8-week-old mice were inoculated in both hind legs in the thigh muscles (dorsal thigh muscle for the right leg and ventral thigh muscles for the left leg) with 1×10^7 infectious particles of RABV. Disease progression was evaluated by scoring clinical signs and mortality as previously described (Chopy et al. 2011) and as follows: 0=normal mice, 1=ruffled fur, 2=one paralyzed hind leg, 3=two paralyzed hind legs and hunched back, 4=tetraplegia (defined as the total loss of mobility), and 5=death (mice were sacrificed when moribund). Data were presented as a cumulative clinical score (the individual clinical score for each mouse was added) and as a mortality curve. In other experiments, groups of mice (at least $n=3$) were deeply anesthetized and intracardially perfused with SPB–$Ca^{2+}Mg^{2+}$. Organs (hindlimb muscles, spinal cord, and brain) were collected separately and stored at −80°C before being processed for RNA or protein extraction.

Ethical statement

Animal housing and experimental protocols followed guidelines approved by the French Ministry of Agriculture and Institut Pasteur Ethical committee. The Institut Pasteur is a member of Le Comité 1 Régional d'Ethique pour l'Expérimentation Animale (CREEA) de l'Ile de France.

Statistical analysis

For comparison of groups, Student's *t* tests were performed using GraphPad Prism version 5.0 for Windows. For the animal experiments, collected data were plotted for comparison in Gehan–Breslow–Wilcoxon test (survival curves) and Wilcoxon matched pairs signed rank test (clinical scores).

Acknowledgments We are grateful to Christophe Préhaud for helpful advice and to the animal keepers from the Institut Pasteur animal facility for breeding the IFNAR$^{-/-}$ mice.

This work was supported by internal grants of Institut Pasteur. Damien Chopy is the recipient of a fellowship from the French Ministère de l'Enseignement Supérieur et de la Recherche.

References

Baloul L, Camelo S, Lafon M (2004) Up-regulation of Fas ligand (FasL) in the central nervous system: a mechanism of immune evasion by rabies virus. J Neurovirol 10:372–382

Blondel D, Kheddache S, Lahaye X, Dianoux L, Chelbi-Alix MK (2010) Resistance to rabies virus infection conferred by the PMLIV isoform. J Virol 84:10719–10726

Brzozka K, Finke S, Conzelmann KK (2005) Identification of the rabies virus alpha/beta interferon antagonist: phosphoprotein P interferes with phosphorylation of interferon regulatory factor 3. J Virol 79:7673–7681

Brzozka K, Finke S, Conzelmann KK (2006) Inhibition of interferon signaling by rabies virus phosphoprotein P: activation-dependent binding of STAT1 and STAT2. J Virol 80:2675–2683

Camelo S, Lafage M, Lafon M (2000) Absence of the p55 Kd TNF-alpha receptor promotes survival in rabies virus acute encephalitis. J Neurovirol 6:507–518

Castellanos JE, Martinez-Gutierrez M, Hurtado H, Kassis R, Bourhy H, Acosta O, Lafon M (2005) Studying neurotrophin antiviral effect on rabies-infected dorsal root ganglia cultures. J Neurovirol 11:403–410

Chelbi-Alix MK, Vidy A, El Bougrini J, Blondel D (2006) Rabies viral mechanisms to escape the IFN system: the viral protein P interferes with IRF-3, Stat1, and PML nuclear bodies. J Interferon Cytokine Res 26:271–280

Chen S, Short JA, Young DF, Killip MJ, Schneider M, Goodbourn S, Randall RE (2010) Heterocellular induction of interferon by negative-sense RNA viruses. Virology 407:247–255

Chopy D, Pothlichet J, Lafage M et al (2011) Ambivalent role of the innate immune response in rabies virus pathogenesis. J Virol 85:6657–6668

Conrady CD, Drevets DA, Carr DJ (2010) Herpes simplex type I (HSV-1) infection of the nervous system: is an immune response a good thing? J Neuroimmunol 220:1–9

D'Agostino PM, Amenta JJ, Reiss CS (2009) IFN-beta-induced alteration of VSV protein phosphorylation in neuronal cells. Viral Immunol 22:353–369

Detje CN, Meyer T, Schmidt H, Kreuz D, Rose JK, Bechmann I, Prinz M, Kalinke U (2009) Local type I IFN receptor signaling protects against virus spread within the central nervous system. J Immunol 182:2297–2304

Faul EJ, Wanjalla CN, McGettigan JP, Schnell MJ (2008) Interferon-beta expressed by a rabies virus-based HIV-1 vaccine vector serves as a molecular adjuvant and decreases pathogenicity. Virology 382:226–238

Faul EJ, Wanjalla CN, Suthar MS et al (2010) Rabies virus infection induces type I interferon production in an IPS-1 dependent manner while dendritic cell activation relies on IFNAR signaling. PLoS Pathog 6:e1001016

Floris S, Ruuls SR, Wierinckx A, van der Pol SM, Dopp E, van der Meide PH, Dijkstra CD, De Vries HE (2002) Interferon-beta directly influences monocyte infiltration into the central nervous system. J Neuroimmunol 127:69–79

Fragkoudis R, Tamberg N, Siu R, Kiiver K, Kohl A, Merits A, Fazakerley JK (2009) Neurons and oligodendrocytes in the mouse brain differ in their ability to replicate Semliki Forest virus. J Neurovirol 15:57–70

Fu ZF, Jackson AC (2005) Neuronal dysfunction and death in rabies virus infection. J Neurovirol 11:101–106

Galelli A, Baloul L, Lafon M (2000) Abortive rabies virus central nervous infection is controlled by T lymphocyte local recruitment and induction of apoptosis. J Neurovirol 6:359–372

Hornung V, Ellegast J, Kim S, Brzozka K, Jung A, Kato H, Poeck H, Akira S, Conzelmann KK, Schlee M, Endres S, Hartmann G

(2006) 5′-Triphosphate RNA is the ligand for RIG-I. Science 314:994–997

Ida-Hosonuma M, Iwasaki T, Yoshikawa T, Nagata N, Sato Y, Sata T, Yoneyama M, Fujita T, Taya C, Yonekawa H, Koike S (2005) The alpha/beta interferon response controls tissue tropism and pathogenicity of poliovirus. J Virol 79:4460–4469

Ireland DD, Stohlman SA, Hinton DR, Atkinson R, Bergmann CC (2008) Type I interferons are essential in controlling neurotropic coronavirus infection irrespective of functional CD8 T cells. J Virol 82:300–310

Ito N, Moseley GW, Blondel D, Shimizu K, Rowe CL, Ito Y, Masatani T, Nakagawa K, Jans DA, Sugiyama M (2010) Role of interferon antagonist activity of rabies virus phosphoprotein in viral pathogenicity. J Virol 84:6699–6710

Jackson AC, Randle E, Lawrance G, Rossiter JP (2008) Neuronal apoptosis does not play an important role in human rabies encephalitis. J Neurovirol 14:368–375

Johnson N, McKimmie CS, Mansfield KL, Wakeley PR, Brookes SM, Fazakerley JK, Fooks AR (2006) Lyssavirus infection activates interferon gene expression in the brain. J Gen Virol 87:2663–2667

Jolly C (2011) Cell-to-cell transmission of retroviruses: innate immunity and interferon-induced restriction factors. Virology 411:251–259

Kuss SK, Etheredge CA, Pfeiffer JK (2008) Multiple host barriers restrict poliovirus trafficking in mice. PLoS Pathog 4:e1000082

Lafon M (2008) Immune evasion, a critical strategy for rabies virus. Dev Biol (Basel) 131:413–419

Lafon M, Wiktor TJ (1985) Antigenic sites on the ERA rabies virus nucleoprotein and non-structural protein. J Gen Virol 66(Pt 10):2125–2133

Lafon M, Prehaud C, Megret F, Lafage M, Mouillot G, Roa M, Moreau P, Rouas-Freiss N, Carosella ED (2005) Modulation of HLA-G expression in human neural cells after neurotropic viral infections. J Virol 79:15226–15237

Lafon M, Megret F, Meuth SG, Simon O, Velandia Romero ML, Lafage M, Chen L, Alexopoulou L, Flavell RA, Prehaud C, Wiendl H (2008) Detrimental contribution of the immuno-inhibitor b7-h1 to rabies virus encephalitis. J Immunol 180:7506–7515

Laothamatas J, Wacharapluesadee S, Lumlertdacha B, Ampawong S, Tepsumethanon V, Shuangshoti S, Phumesin P, Asavaphatiboon S, Worapruekjaru L, Avihingsanon Y, Israsena N, Lafon M, Wilde H, Hemachudha T (2008) Furious and paralytic rabies of canine origin: neuroimaging with virological and cytokine studies. J Neurovirol 14:119–129

Lodmell DL, Wiedbrauk DL, Ewalt LC (1989) Interferon induced within the central nervous system during infection is inconsequential as a mechanism responsible for murine resistance to street rabies virus. J Gen Virol 70(Pt 2):473–478

Marcovistz R, Germano PM, Riviere Y, Tsiang H, Hovanessian AG (1987) The effect of interferon treatment in rabies prophylaxis in immunocompetent, immunosuppressed, and immunodeficient mice. J Interferon Res 7:17–27

Masatani T, Ito N, Shimizu K et al (2010a) Amino acids at positions 273 and 394 in rabies virus nucleoprotein are important for both evasion of host RIG-I-mediated antiviral response and pathogenicity. Virus Res 155:168–174

Masatani T, Ito N, Shimizu K, Ito Y, Nakagawa K, Sawaki Y, Koyama H, Sugiyama M (2010b) Rabies virus nucleoprotein functions to evade activation of the RIG-I-mediated antiviral response. J Virol 84:4002–4012

McFadden G, Mohamed MR, Rahman MM, Bartee E (2009) Cytokine determinants of viral tropism. Nat Rev Immunol 9:645–655

Menager P, Roux P, Megret F, Bourgeois JP, Le Sourd AM, Danckaert A, Lafage M, Prehaud C, Lafon M (2009) Toll-like receptor 3 (TLR3) plays a major role in the formation of rabies virus Negri Bodies. PLoS Pathog 5:e1000315

Muller U, Steinhoff U, Reis LF, Hemmi S, Pavlovic J, Zinkernagel RM, Aguet M (1994) Functional role of type I and type II interferons in antiviral defense. Science 264:1918–1921

Pfeiffer JK (2010) Innate host barriers to viral trafficking and population diversity: lessons learned from poliovirus. Adv Virus Res 77:85–118

Prehaud C, Megret F, Lafage M, Lafon M (2005) Virus infection switches TLR-3-positive human neurons to become strong producers of beta interferon. J Virol 79:12893–12904

Prehaud C, Wolff N, Terrien E, Lafage M, Megret F, Babault N, Cordier F, Tan GS, Maitrepierre E, Menager P, Chopy D, Hoos S, England P, Delepierre M, Schnell MJ, Buc H, Lafon M (2010) Attenuation of rabies virulence: takeover by the cytoplasmic domain of its envelope protein. Sci Signal 3:ra5

Prinz M, Schmidt H, Mildner A, Knobeloch KP, Hanisch UK, Raasch J, Merkler D, Detje C, Gutcher I, Mages J, Lang R, Martin R, Gold R, Becher B, Bruck W, Kalinke U (2008) Distinct and nonredundant in vivo functions of IFNAR on myeloid cells limit autoimmunity in the central nervous system. Immunity 28:675–686

Raaben M, Groot Koerkamp MJ, Rottier PJ, de Haan CA (2009) Type I interferon receptor-independent and -dependent host transcriptional responses to mouse hepatitis coronavirus infection in vivo. BMC Genomics 10:350

Rieder M, Conzelmann KK (2009) Rhabdovirus evasion of the interferon system. J Interferon Cytokine Res 29:499–509

Rieder M, Brzozka K, Pfaller CK, Cox JH, Stitz L, Conzelmann KK (2011) Genetic dissection of interferon-antagonistic functions of rabies virus phosphoprotein: inhibition of interferon regulatory factor 3 activation is important for pathogenicity. J Virol 85:842–852

Sadler AJ, Williams BR (2008) Interferon-inducible antiviral effectors. Nat Rev Immunol 8:559–568

Scott CA, Rossiter JP, Andrew RD, Jackson AC (2008) Structural abnormalities in neurons are sufficient to explain the clinical disease and fatal outcome of experimental rabies in yellow fluorescent protein-expressing transgenic mice. J Virol 82:513–521

Shimizu K, Ito N, Sugiyama M, Minamoto N (2006) Sensitivity of rabies virus to type I interferon is determined by the phosphoprotein gene. Microbiol Immunol 50:975–978

Steinhoff U, Muller U, Schertler A, Hengartner H, Aguet M, Zinkernagel RM (1995) Antiviral protection by vesicular stomatitis virus-specific antibodies in alpha/beta interferon receptor-deficient mice. J Virol 69:2153–2158

Thoulouze MI, Lafage M, Montano-Hirose JA, Lafon M (1997) Rabies virus infects mouse and human lymphocytes and induces apoptosis. J Virol 71:7372–7380

Torres-Anjel MJ, Volz D, Torres MJ, Turk M, Tshikuka JG (1988) Failure to thrive, wasting syndrome, and immunodeficiency in rabies: a hypophyseal/hypothalamic/thymic axis effect of rabies virus. Rev Infect Dis 10(Suppl 4):S710–S725

Trinchieri G (2010) Type I interferon: friend or foe? J Exp Med 207:2053–2063

Trottier MD Jr, Palian BM, Reiss CS (2005) VSV replication in neurons is inhibited by type I IFN at multiple stages of infection. Virology 333:215–225

Veldhuis WB, Floris S, van der Meide PH, Vos IM, de Vries HE, Dijkstra CD, Bar PR, Nicolay K (2003) Interferon-beta prevents cytokine-induced neutrophil infiltration and attenuates blood–brain barrier disruption. J Cereb Blood Flow Metab 23:1060–1069

Vercammen E, Staal J, Beyaert R (2008) Sensing of viral infection and activation of innate immunity by toll-like receptor 3. Clin Microbiol Rev 21:13–25

Vidy A, Chelbi-Alix M, Blondel D (2005) Rabies virus P protein interacts with STAT1 and inhibits interferon signal transduction pathways. J Virol 79:14411–14420

Vidy A, El Bougrini J, Chelbi-Alix MK, Blondel D (2007) The nucleocytoplasmic rabies virus P protein counteracts interferon signaling by inhibiting both nuclear accumulation and DNA binding of STAT1. J Virol 81:4255–4263

Wang ZW, Sarmento L, Wang Y, Li XQ, Dhingra V, Tseggai T, Jiang B, Fu ZF (2005) Attenuated rabies virus activates, while pathogenic rabies virus evades, the host innate immune responses in the central nervous system. J Virol 79:12554–12565

Zhao L, Toriumi H, Kuang Y, Chen H, Fu ZF (2009) The roles of chemokines in rabies virus infection: overexpression may not always be beneficial. J Virol 83:11808–11818